Belgirate, Italy, 28-30 September 2005

AN APPROACH TO THE ELECTRICAL CHARACTERIZATION OF ANALOG BLOCKS THROUGH THERMAL MEASUREMENTS

Diego Mateo, Josep Altet, and Eduardo Aldrete-Vidrio

Electronic Engineering Department, Universitat Politècnica de Catalunya, Barcelona, Spain
{mateo, pepaltet, aldrete}@eel.upc.edu

ABSTRACT

In this work the authors analyse the effects of the electrical performances of analogue circuits, specifically amplifiers, on the silicon surface thermal map. The goal of this analysis is to explore the feasibility of obtaining the figures of merit of analogue blocks from temperature measurements.

1. INTRODUCTION

The scaling down of CMOS technologies and its benefits on circuits performances has enabled the possibility of integrating a whole system on a single silicon chip, with the benefits of low cost, high reliability, low power consumption, etc. Nevertheless, this System on Chip (SoC) integration suffers from a significant loss in terms of observability, since fewer nodes are accessible from the outside. This loss of observability increases the complexity of the test and characterization of the individual parts of the system.

Paradigms of SoC are the nowadays so well-known RF wireless communication systems. Figure 1 shows a typical block diagram of a RF receiver: Low Noise Amplifier (LNA), Mixer, Voltage Controlled Oscillator (VCO), Filter and Analogue to Digital Converter (ADC). The connections between the different blocks are not always accessible and, therefore, extracting the figures of merit of the different individual blocks (i.e., gain, non-linearity, phase noise...) is not a straightforward task.

In order to increase the observability of the different blocks, we are currently investigating the possibility of extracting the electrical performances of the different analogue blocks from temperature measurements carried out on the silicon surface. For instance, Figure 1 indicates the points where temperature would be measured (Temperature Observation Points).

This paper addresses some of the challenges that this research presents, e.g., thermal coupling in the silicon surface has a limited bandwidth. Section 2 discusses how to map the high frequency electrical figures of merit (for instance, the gain at 2.4 GHz of an amplifier) into low frequency components (less than 1 MHz) of the power dissipated by some devices of the circuit. Section 3 details the number of spectral components thermally observable and the dependence of their magnitude on the electrical performances of an amplifier: gain and non-linearity of second and third order.

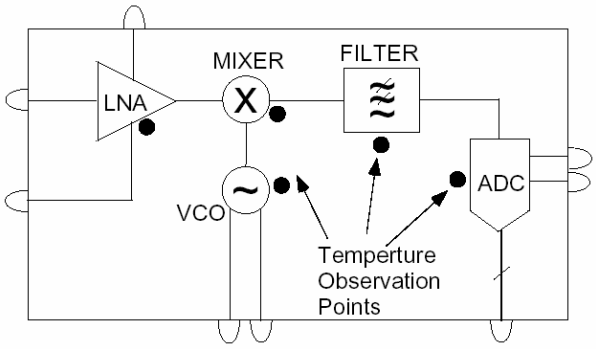

Figure 1: Block diagram of a RF receiver.

The feasibility of measuring the power dissipated by some integrated devices by measuring its temperature has been shown elsewhere, either using laser techniques [2] or integrated temperature sensors [3, 4].

By using a built-in differential temperature sensor, section 4 describes some experimental results that show the feasibility of the thermal measurements proposed in the previous sections. Finally, the conclusions of the work are summarized in section 5.

2. ELECTRICAL CHARACTERIZATION BY THERMAL MEASUREMENT

An important electrical characteristic of any analogue block is its gain. Let us consider an amplifier with an ideal relation between input, V_{in}, and output, V_{out}:

$$V_{out} = K_1 \cdot V_{in} \tag{1}$$

And let us apply two tones at the input to analyze the output. With the ideal behaviour shown in the previous equation, the spectral content of the voltage at the output is just a scaled version of the input by the gain K_1.

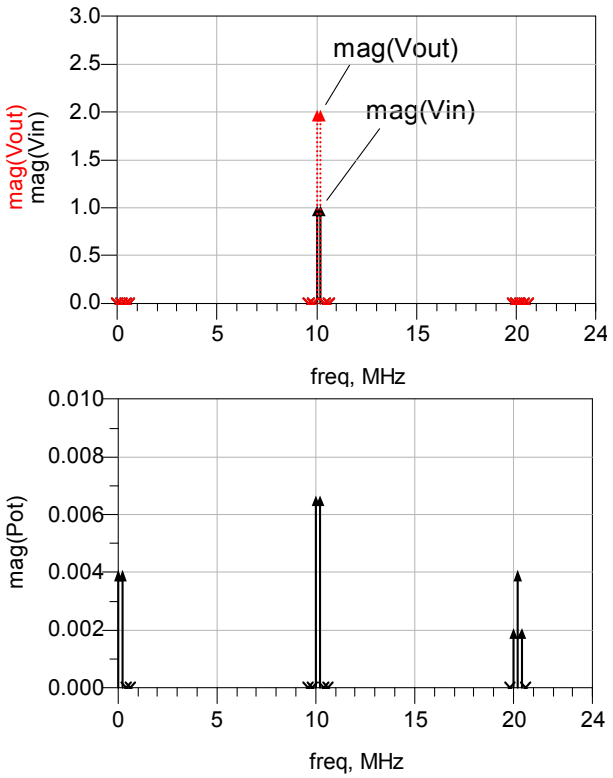

Figure 2: Spectrum of (a) input and output voltages [V], and (b) dissipated power [W].

Figure 2.a shows two input tones at f_1 = 10 MHz and f_2 = 10.1 MHz with unitary amplitude that have been considered at the input, when the amplifier has a gain of K_1 = 2. But if we look at the dissipated power (see Figure 2.b, where in order to have some power dissipated we assume a certain output impedance), its spectrum contains more frequencies than that corresponding to the voltage. Specifically, there is some power dissipated at f_2 - f_1 = 100 KHz, and it is easy to find that it depends on the gain K_1.

If the output is not accessible then it will be impossible to characterize the amplifier externally. If the main frequencies are in the order of hundreds of MHz or few GHz (usual values in RF wireless communications systems), it will be also impossible to measure the temperature corresponding to dissipations at this so high frequencies (some works have reported thermal measurements corresponding to powers dissipated up to 100 KHz [3]). But if f_2 - f_1 is small enough, it will be possible to estimate the power dissipated at this low frequency, which as we show in next section is related to the gain of the amplifier. In this simple example we base the main idea of the work: electrical characterization of non-observable analogue blocks working at high frequencies through thermal measurement of the power dissipated at low frequencies by some of its dissipative devices. In addition, not only the gain can be estimated, but also non-linearities: if we consider a non-linear behaviour of the amplifier, modelled for example by a power series up to the second order given by,

$$V_{out} = K_1 \cdot V_{in} + K_2 \cdot V_{in}^2 \qquad (2)$$

Then in such a case, the spectral content of the dissipated power shows even more tones due to the non-linearity (see Figure 3), with the same values as before plus $K_2 = 1\text{V}^{-1}$, where now there is also power dissipated at $2(f_2 - f_1)$.

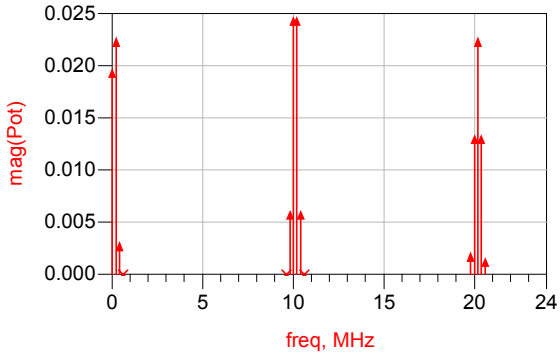

Figure 3: Spectrum of the dissipated power with some non-linear behaviour [W].

3. EFFECTS OF THE ELECTRICAL PERFORMANCES ON POWER DISSIPATION

The goal of this section is to characterize mathematically the power dissipated by the devices of an amplifier as a function of its electrical performances of gain and non-linearity. Specifically, we will concentrate the analysis on the spectral components of the power dissipated that may cause thermal coupling in the silicon die and that are susceptible of being measured with built-in temperature sensors. Figure 4 shows the simplified model of the amplifier considered in this section.

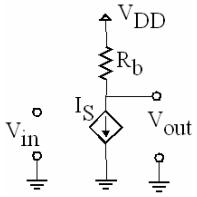

Figure 4: Simplified model of the considered amplifier.

The voltage controlled current source models the active device (usually a MOS transistor), whereas the resistor R_b models the load. The current I_S provided by the source can be written in general as:

$$I_S = I_{DC} + f(V_{in}) \qquad (3)$$

where I_{DC} is the bias current and $f(V_{in})$ is a transconductance function. Three different transconductance functions are considered in this paper:

$$f(V_{in}) = K_1 \cdot V_{in} \quad (4)$$

$$f(V_{in}) = K_1 \cdot V_{in} + K_2 \cdot V_{in}^2 \quad (5)$$

$$f(V_{in}) = K_1 \cdot V_{in} + K_2 \cdot V_{in}^2 + K_3 \cdot V_{in}^3 \quad (6)$$

Expression (4) models an ideal linear amplifier, whereas expressions (5) and (6) model the second and third order non-linearities. We analyse next the power dissipated by the active device considering that a sum of tones are applied at the input of the amplifier:

$$V_{in} = A \cdot \sum_{i=1}^{N} \cos(\omega_i \cdot t) \quad (7)$$

where A is the amplitude of the tones, and $\omega_i = 2\pi f_i$ are the i-different frequencies. In this paper cases of $N = 1$ and $N = 2$ are considered. We assume that the frequency of the input tones is beyond the cut-off frequency of the thermal coupling that may exist between devices in the silicon die, e.g., the amplifier is a typical RF amplifier working in the ISM band (2.4 GHz). We also assume that the tones applied are "close enough" between them (f_1, f_2 >> $|f_1 - f_2|$), in such a way that their differences (and some multiples of them) are thermally observable. Let's name P_s to the power dissipated by the active device, which can be expressed as:

$$P_S = V_{DD} \cdot I_S - I_S^2 \cdot R_b \quad (8)$$

Table 1 (see next page) summarizes the main results of the analysis performed in this section. Depending on the amplifier analyzed (ideal or with non-linearities), the table is divided in three sections. In left column, N is the number of tones applied to the input of the amplifier. From all the spectral components of the power dissipated by the active device, in column *Freq.* we list the frequencies that are thermally observable. Expression in column *Power amplitude expression* shows the amplitude of the specific spectral component of the dissipated power.

For example, let's concentrate from now on, in the model of the amplifier with second order non-linearity with two tones applied at its input. If we analyse the dissipated power, we will find that it has components at the following frequencies: *DC,* ω_1-ω_2, $2\omega_1$-$2\omega_2$, ω_1, ω_2, $\omega_1+\omega_2$, $2\omega_1-\omega_2$, $2\omega_2-\omega_1$, $2\omega_1$, $2\omega_2$, $2\omega_1+\omega_2$, $\omega_1+2\omega_2$, $2\omega_1+2\omega_2$, $3\omega_1$, $3\omega_2$, $3\omega_1-\omega_2$, $3\omega_2-\omega_1$, $3\omega_1+\omega_2$, $\omega_1+3\omega_2$, $4\omega_1$ and $4\omega_2$.

However, with the hypothesis previously made, only three components of this power will be thermally observable (*DC,* ω_1-ω_2, and $2\omega_1$-$2\omega_2$), which appear in the *Freq.* column, when $N=2$. If we name P_t to the addition of these three components, then:

$$P_t = P_{DC} + P_1 \cos((\omega_1 - \omega_2) \cdot t) + P_2 \cos((2\omega_1 - 2\omega_2) \cdot t) \quad (9)$$

where

$$P_{DC} = V_{DD} I_{DC} - R_b I_{DC}^2 - R_b K_1^2 A^2 + V_{DD} K_2 A^2 - 2R_b I_{DC} K^2 A^2 - \frac{9}{4} R_b K_2^2 A^4 \quad (10)$$

$$P_1 = -R_b K_1^2 A^2 + V_{DD} K_2 A^2 - 3R_b K_2^2 A^4 - 2R_b I_{DC} K^2 A^2 \quad (11)$$

$$P_2 = -\frac{3}{2} R_b K_2^2 A^4 \quad (12)$$

In Table 1, the values of P_{DC}, P_1 and P_2 are the power amplitudes of the spectral components at frequencies *DC,* ω_1-ω_2, and $2\omega_1$-$2\omega_2$, respectively, and they appear in column *Power amplitude expression*. Terms are grouped in parenthesis to help in identifying which is the origin of the power dissipation: DC bias, the linear gain or the non-linearity coefficients.

Let us now comment the contents of Table 1. In an ideal linear amplifier (K_2 and K_3 equal to zero) with $N = 1$, there is no signal (voltage or current) at other frequencies than those applied at the input, ω_1 and ω_2. But the non-linear behaviour of the dissipated power (it is calculated as the *Voltage* per *Current* product) provokes a translation in frequency, having then power dissipated at (ω_1-ω_2). We call to this frequency translation *mixing effect.* As it is shown in Table 1, the magnitude of this power depends only on the gain K_1, being then possible to derive the gain from thermal measurements in such a linear case.

With $N = 2$, if the amplifier has some non-negligible second order non-linearity, there will be some voltages and/or currents in the amplifier at other frequencies than those applied at the input, basically at frequencies (ω_1-ω_2) and (ω_1+ω_2). And because of the DC biasing, there will be another contribution to the dissipated power at those frequencies. In this case, the power dissipated at (ω_1-ω_2) due to the mixing effect is:

$$(-R_b \cdot K_1^2 \cdot A^2) - (3 \cdot R_b \cdot K_2^2 \cdot A^4) \quad (13)$$

whereas the power dissipated due to the electrical signals present in the circuit at this frequency is given by:

$$(V_{DD} \cdot K_2 \cdot A^2 - 2 \cdot R_b \cdot I_{DC} \cdot K_2 \cdot A^2) \quad (14)$$

Table 1: Power amplitude expressions for the different cases considered.

N	Freq.	Power amplitude expressions of this frequency spectral component.
Model: Ideal lineal (equation: $I_S = I_{DC} + K_1 \cdot V_{in}$)		
N=1	DC	$\left(V_{DD} \cdot I_{DC} - R_b \cdot I_S^2\right) - \left(\frac{1}{2} \cdot R_b \cdot K_1^2 \cdot A^2\right)$
N=2	DC	$\left(V_{DD} \cdot I_{DC} - R_b \cdot I_{DC}^2\right) - \left(R_b \cdot K_1^2 \cdot A^2\right)$
	ω_1-ω_2	$\left(- R_b \cdot K_1^2 \cdot A^2\right)$
Model: Amplifier with second order non-linearity (equation: $I_S = I_{DC} + K_1 \cdot V_{in} + K_2 \cdot V_{in}^2$)		
N=1	DC	$\left(V_{DD} \cdot I_{DC} - R_b \cdot I_{DC}^2\right) - \left(\frac{1}{2} R_b \cdot K_1^2 \cdot A^2\right) + \left(\frac{1}{2} V_{DD} \cdot K_2 \cdot A^2 - R_b \cdot I_{DC} \cdot K_2 \cdot A^2 - \frac{3}{8} \cdot R_b \cdot K_2^2 \cdot A^4\right)$
N=2	DC	$\left(V_{DD} \cdot I_{DC} - R_b \cdot I_{DC}^2\right) - \left(R_b \cdot K_1^2 \cdot A^2\right) + \left(V_{DD} \cdot K_2 \cdot A^2 - 2 \cdot R_b \cdot I_{DC} \cdot K_2 \cdot A^2 - \frac{9}{4} \cdot R_b \cdot K_2^2 \cdot A^4\right)$
	ω_1-ω_2	$\left(-R_b \cdot K_1^2 \cdot A^2\right) + \left(V_{DD} \cdot K_2 \cdot A^2 - 3 \cdot R_b \cdot K_2^2 \cdot A^4 - 2 \cdot R_b \cdot I_{DC} \cdot K_2 \cdot A^2\right)$
	$2\omega_1$-$2\omega_2$	$-\frac{3}{4} R_b \cdot K_2^2 \cdot A^4$
Model: Amplifier with second and third order non-linearity (equation: $I_S = I_{DC} + K_1 \cdot V_{in} + K_2 \cdot V_{in}^2 + K_3 \cdot V_{in}^3$)		
N=1	DC	$\left(V_{DD} I_{DC} - R_b I_{DC}^2\right) - \left(\frac{1}{2} R_b K_1^2 A^2\right) + \left(\frac{1}{2} V_{DD} K_2 A^2 - R_b I_{DC} K_2 A^2 - \frac{3}{8} R_b K_2^2 A^4\right) + \left(-\frac{3}{4} R_b K_1 K_3 A^4 - \frac{5}{16} R_b K_3^2 A^6\right)$
N=2	DC	$\left(V_{DD} \cdot I_{DC} - R_b \cdot I_{DC}^2\right) - \left(R_b \cdot K_1^2 \cdot A^2\right) + \left(V_{DD} \cdot K_2 \cdot A^2 - 2 \cdot R_b \cdot I_{DC} \cdot K_2 \cdot A^2 - \frac{9}{4} \cdot R_b \cdot K_2^2 \cdot A^4\right) - \left(\frac{25}{4} \cdot R_b \cdot K_3^2 \cdot A^6 + \frac{9}{2} \cdot R_b \cdot K_1 \cdot K_3 \cdot A^4\right)$
	ω_1-ω_2	$\left(-R_b K_1^2 A^2\right) + \left(V_{DD} K_2 A^2 - 3 R_b K_2^2 A^4 - 2 R_b I_{DC} K_2 A^2\right) + \left(-6 R_b I_{DC} K_1 K_3 A^4 - \frac{75}{8} R_b K_3^2 A^6\right)$
	$2\omega_1$-$2\omega_2$	$\left(-\frac{3}{4} R_b \cdot K_2^2 \cdot A^4\right) + \left(-\frac{15}{4} R_b \cdot K_3^2 \cdot A^6 - \frac{3}{2} R_b \cdot K_3 \cdot K_1 \cdot A^4\right)$
	$3\omega_1$-$3\omega_2$	$-\frac{5}{8} R_b \cdot K_3^2 \cdot A^6$

Then the power dissipated at (ω_1-ω_2) depends on the gain K_1 and also on the second order non-linearity K_2. Nevertheless, the power dissipated at ($2\omega_1$-$2\omega_2$) depends only on K_2. If higher levels of non-linearities are considered, for example K_3, the same analysis applies: power dissipated at ($3\omega_1$-$3\omega_2$) will depend only on K_3, whereas powers dissipated at (ω_1-ω_2) and ($2\omega_1$-$2\omega_2$) depend on K_1, K_2 and K_3.

To illustrate the example of this section with some numerical values, let's suppose an amplifier with R_b = 1KΩ, V_{DD} = 3.3V and I_S = 1.65mA. This sets the operating point of V_{out} to V_{DD}/2. With this R_b value, to have a gain of 10 a nominal value of K_1 = 0.01 is needed. An amplitude of A = 100mV for the input tones will give an output swing of $2V_{pp}$. In a scenario where a 20% of variability in the coefficient K_1 is assumed, and using the model of the ideal amplifier, the value of the power amplitudes of the *DC* (top) and (ω_1-ω_2 (bottom) spectral components are shown in Figure 5.

Figure 6 shows the amplitudes of the spectral components of the dissipated power, (ω_1-ω_2) (top) and ($2\omega_1$-$2\omega_2$) (bottom), considering that the amplifier has a second order non-linearity which may go from 0.0011 V^{-1} to 0.021 V^{-1}.

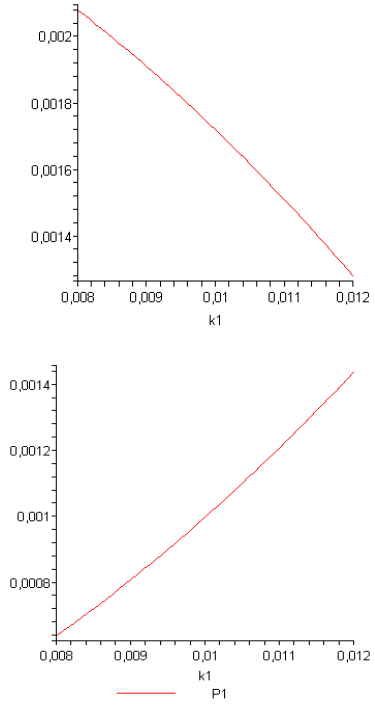

Figure 5: Ideal amplifier: power dissipated at DC (top), and (ω_1-ω_2) (bottom), [W].

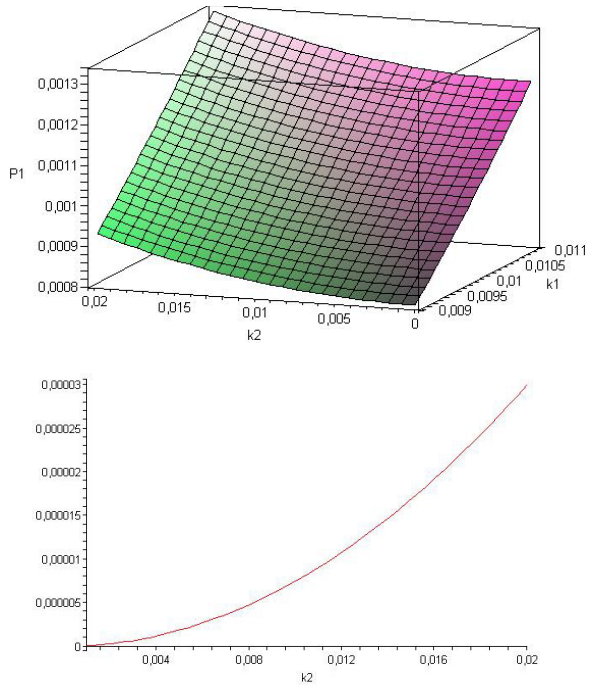

Figure 6: dissipation at (ω_1-ω_2) (top) and ($2\omega_1$-$2\omega_2$) (bottom) for a 2nd order non-linearity, [W].

From all these figures we can observe that there is certainly an important dependence of the power dissipated by the active device on the electrical performances of the amplifier.

4. MEASURING THE TEMPERATURE: DISCUSSION AND EXAMPLE

Different techniques for measuring the dynamic evolution of the temperature on the silicon surface have been reported in the literature, which can be categorized as non-contact [4] (e.g., reflectometry and interferometry) and built-in techniques [5].

The objective of the experimentation presented in this section is to show the feasibility of detecting the power dissipated by a heat source at the frequencies of the intermodulation products that appear when two tones are applied to that heat source. Figure 7 shows the set-up used for the experimental data reported in this section.

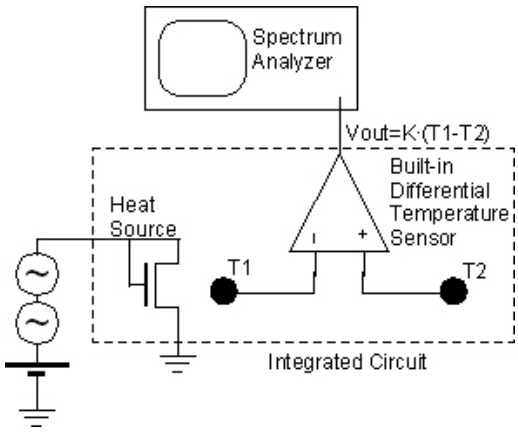

Figure 7: Set-up used for the experimentation.

The integrated circuit is formed by MOS transistors working as heat sources and a built-in differential temperature sensor. The differential temperature sensor gives an output voltage proportional to the difference of temperature at two points of the silicon surface. This sensor circuit has been implemented in a 1.2 microns technology and it has been used in many works reported in the literature (e.g., [4, 5, 6]). Its sensitivity is about 2.4 V/ºC. In our case, the distance between the two temperature monitoring points, T_1 and T_2, is 500 microns, whereas the distance between the heat source and the temperature monitoring point T_1 ranges from 17 microns till 150 microns, depending on which of the heat sources is activated.

As indicated in Figure 7, the active heat source is driven with a DC bias of 3.8V plus two sinusoidal voltages of 0.6*Vpeak*. The output of the sensor has been connected either to an oscilloscope or to a spectrum analyzer.

Figure 8 shows the spectrum of the sensor's output signal. The frequencies of the two tones are 1 KHz and 1.130 KHz. Thus, the separation between them is 130 Hz (multiples of 50 Hz have been avoided).

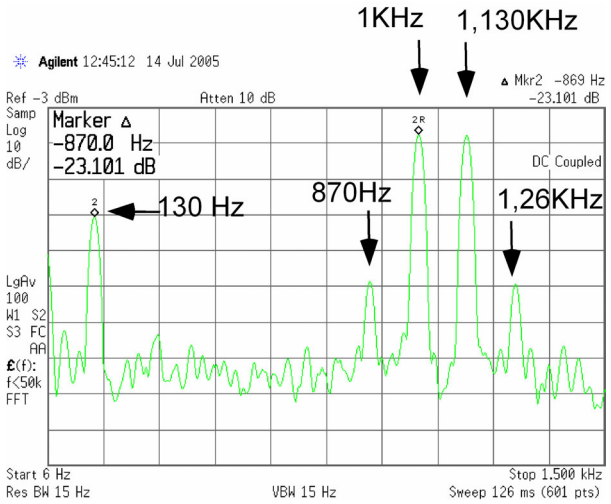

Figure 8: Spectrum of the sensor's output voltage. Frequency of the input tones: 1 KHz and 1.130 KHz

As now the input tones are in the bandwidth of the thermal coupling, they appear in the output sensor spectrum (they are the largest tones in Figure 8). The other spectral components that appear are the intermodulation products: $f_1 - f_2$ (130 Hz), $2f_1 - f_2$ (870 Hz) and $2f_2 - f_1$ (1.26 KHz).

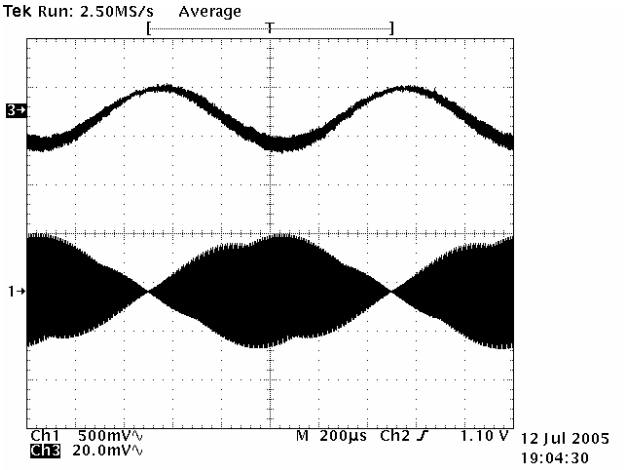

Figure 9: Output of the sensor in the time domain (top). Frequency of the input tones: $f_1 = 100$ KHz, $f_2 = 101$ KHz (bottom)

Figure 9 shows the output of the sensor in the time domain (top signal) when the heat source has been activated with two tones with frequencies of 100 KHz and 101 KHz. The bottom signal is the input signal. As it can be seen, the main frequency at the sensor's output is 1 KHz, with some higher frequency components corresponding to the input tones superposed to it. Due to the properties of the thermal coupling, these higher frequency tones suffer from higher attenuation.

5. CONCLUSIONS

In the present paper the authors have analysed the relation between specific low frequency spectral components of the power dissipated in the active device of an amplifier, and some electrical performances of the amplifier at high frequencies. Specifically, we have analysed the effects of gain and second and third order non-linearities. The final goal is to use this relationship to derive the electrical performances of analogue and RF circuits at high frequencies from estimations of the dissipated power at low frequencies. These estimations will be done by thermal measurements; as such thermal measurements have the added benefit of not loading electrically the circuit to characterize.

The experimental results show the feasibility of measuring different spectral components of the temperature dissipated by a device by using temperature sensors built-in with the dissipating device.

ACKNOWLEDGEMENTS

This work has been partially supported by the project TEC2004-03289 and the Research Grants (AGAUR) 2005FIR 00080.

REFERENCES

[1] W. Shen, B. Xia, A. Emira, C. Sin, A. Y. Valero-López, S. T. Moon, and E, Sánchez Sinencio, "A 3-V, 0.35um CMOS Bluetooth Receiver IC", *IEEE Journal of Solid State Circuits*, vol. 38, no. 1, pp. 30-42, January 2003.

[2] W. Claeys, S. Dilhaire, S. Jorez, and L.-D. Patiño-Lopez, "Laser probes for the thermal and thermomechanical characterisation of microelectronic devices," *Microelectronics Journal*, vol. 32, no. 10-11, pp: 891-898, October-November 2001.

[3] N. Nenadovic, S. Mijalkovic, L.K. Nanver, L.J.K. Vandamme, H. Schellevis, V. d'Alessandro, J.W. Slotboom, "Extraction and modelling of self-heating and mutual thermal coupling impedance of bipolar transistors," *in Proceedings of the Bipolar/BiCMOS Circuits and Technology Meeting*, 2003, pp: 125-128, 28-30 September 2003.

[4] J. Altet, S. Dilhaire, S. Volz, J.-M. Rampnoux, A. Rubio, S. Grauby, L. D. Patino Lopez, W. Claeys, and J.-B. Saulnier "Four different approaches for the measurement of IC surface temperature: application to thermal testing," *Microelectronics Journal*, vol. 33, no. 9, pp: 689-696, September 2002.

[5] J. Altet, A. Rubio, S. Dilhaire, E. Schaub, W. Claeys, "BiCMOS thermal sensor circuit for built-in test purposes," *Electronics Letters* vol. 34, no. 13, 25 pp: 1307-1309, June 1998.